Green Chemistry

Eco-foaming Lignin for Innovative Rigid Foams

Journal:	*Green Chemistry*
Manuscript ID	GC-ART-12-2023-005123.R1
Article Type:	Paper
Date Submitted by the Author:	03-Feb-2024
Complete List of Authors:	Yan, Qiangu; USDA Forest Products Laboratory, Forest Products Lab Ketelboeter, Timothy; USDA Forest Products Laboratory, Forest Products Lab Fan, Wenjun; University of Missouri, Department of Chemical and Biomedical Engineering Wan, Caixia; University of Missouri, Chemical and Biomedical Engineering Cai, Zhiyong; USDA Forest Products Laboratory

Eco-foaming Lignin for Innovative Rigid Foams

Qiangu Yan [a], Timothy Ketelboeter [a], Wenjun Fan[a], Caixia Wan [b, *], and Zhiyong Cai [a, *]

[a] Forest Products Lab, USDA Forest Service, One Gifford Pinchot Drive, Madison, WI 53726-2398

[b] Department of Chemical and Biomedical Engineering, University of Missouri, 1406 East Rollins Street, Columbia, MO 65211

[*]Corresponding authors. Tel: +1 573 884 7882, Email: wanca@missouri.edu (Caixia Wan); Tel: +1 608-231-9446, Email: zhiyong.cai@usda.gov (Zhiyong Cai).

Abstract

Rigid lignin foams were prepared by a baking method using kraft lignin as the sole resource. The preparation process involved cold-pressing kraft lignin powder into a solid block, heating the solid block to form a lignin foam, and finally curing and cooling the lignin foam to obtain an open-cell, rigid foam. Both the adsorbed water and water generated from dehydration of hydroxyl groups in the lignin served as the blowing agent in this baking method. It was found that as the moisture contents of lignin decreased, the foam densities increased, the mean bubble size decreased, and the bubble size distribution became narrower. Foam morphology showed an open cell structure and a wide cell volume distribution. The results suggest that controlling the moisture content in raw lignin allows for control of the pore structure of the lignin foam. Based on their unique properties, the lignin foam materials have great promise in many applications especially for core insulation materials of structural insulated panels (SIPs).

Keywords: Rigid lignin foams, kraft lignin, baking process, cold press, open cell.

1. Introduction

Lignin, a major component of lignocellulosic biomass and the most abundant naturally occurring aromatic polymer, has been reported to make foam composites for insulation materials. Those foams serve as green alternatives to replace counterparts based on petrochemicals (mainly polystyrene (PS)) or inorganics (e.g., glass and rock wools)[1]. In addition to insulation, rigid foam boards also provide structural strength, increase thermal break, provide exterior sheathing, and serve as an air barrier [1, 2]. If successfully exploited, lignin-based foam would open huge market opportunities for technical lignin. Approximately 70 million metric tons of technical lignin is produced annually worldwide [3], and cost-effective utilization of lignin is an integral part of lignin valorization to ensure profitable pulping and biorefinery industries. There are several problems to be addressed in developing lignin-based foams. Traditionally, lignin formulated into a rigid foam is either as a reactant in the formation of foams such as polyurethane foam or as a filler to increase mechanical strength. Typically, lignin-containing rigid foams contain less than 37% lignin [4]. Such lignin derived foam products may not be either eco-manufactured or fully biodegradable. Thus, we have been motivated to develop 100% lignin-based foam (so-called lignofoam) via baking method. This method is a non-catalytic, single-step foaming process proven effective for making open-cell rigid foam with great promise for structural insulated panel (SIP) core material. In our prior study[5], we fabricated carbon foams with high mechanical strength, excellent thermal conductivity, and super fire resistance via simultaneous lignin foaming and carbonization at the temperature of 400-600 °C under atmospheric pressure followed by further carbonization/graphitization at the elevated temperature of 700-1000 °C under an inert atmosphere. Although this process involved lignin foaming via baking, lignin experienced carbonization at both stages. Lignin foaming at a relatively low temperature for noncarbonized foam products have been

reported so far. Moreover, foaming mechanisms have not been studied in depth, fundamental factors controlling foaming have not been well identified, and no guidance is available for rational design of lignofoam.

The main objective of this work was to investigate the role of moisture/water in foaming of lignin. Moisture was found to play a key role in determining foam cell structure, and mechanical properties. The foam synthesized under the optimal conditions showed excellent structural and mechanical properties and good thermal insulation properties for SIP applications. This work provides useful guidance for manufacturing lignin-based foams and improving their performance.

2. Materials and methods

2.1. Lignin feedstock

Kraft lignin (BioChoice®, Plymouth, NC, USA) was supplied by Domtar Inc. As received, this kraft lignin contained 28-35 wt% water. The lignin was first dried in air at room temperature for 4 weeks and labeled as KL25 with 7.4% moisture. The air-dried lignin (KL25) was further dried at 50, 75, 100, 125, and 150 °C to reach the respective moistures of 4.5%, 2.2%, 1.4%, and 0.5%, and 0%, denoted as KL50, KL75, KL100, KL125, and KL150, respectively.

2.2. Preparation of lignin foams (LFs)

A process for fabrication of lignin foams from kraft lignin was developed and consists of two main steps (Scheme 1): (1) cold-pressing lignin powder into a solid block, and (2) foaming of the lignin block. Three hundred grams of kraft lignin was put into a kitchen blender and crushed for 2 minutes. The lignin powder was then transferred to a mold as detailed in our prior studies [6]. A metal plate was placed in the mold on the top of the lignin powder and the lignin was cold pressed under a pressure up to 650 psi. The mold containing the pressed lignin block was transferred to a Thermo Scientific Heratherm OMH750 Advanced Lab Oven (Thermo Electron

LED GmbH, Langenselbold, Germany). The oven was then heated at a rate of 10 °C/min to 240 °C and held for 60 minutes. After baking, the mold was allowed to cool naturally down to room temperature. This process resulted in the formation of an open celled lignin foam. The foam samples prepared using kraft lignin dried at their respective temperatures were denoted as LF25, LF50, LF75, LF100, LF125, and LF150.

2.3. Characterization

Moisture contents of lignin samples were analyzed following ASTM E871 method using a Mettler Toledo HE73 moisture analyzer. The ATR-FTIR spectra were acquired on Thermo Scientific ATR-FTIR spectrometer (Thermo Scientific, Nicolet iZ10) at a resolution of 4 cm^{-1} for 64 scans in the 500 to 4000 cm^{-1} range. Thermal properties of the samples were analyzed using a Mettler-Toledo TGA/DSC3+ system (Mettler-Toledo, LLC. Columbus, OH, USA). SEM images were recorded over a Zeiss EVO 50 microscopy (Jena, Germany). Pore size distribution, porosity, and average pore size of lignin foams (LF25-LF125) were analyzed based on SEM images using ImageJ software. Compressive strength of lignin foams was analyzed following ASTM C365[7] using an INSTRON 5869 mechanical testing machine, and the foams were cut into 25.4 × 25.4 × 12.5 mm^3 for testing. Thermal insulation properties of lignin foam was measured using a Hot Disk TPS 1500 thermal constants analyzer (ThermTest, Fredericton, NB, Canada) following the ISO/DIS 22007-2.2 standard method [8].

3. Results and Discussion

3.1. Structure changes of lignin during steam-induced foaming

Since the lignin foaming process is mainly caused by steam, the FTIR bands related to adsorbed water and hydroxyl groups in kraft lignin are of most interest. There are 7 bands at 3700-3000 cm^{-1} related to adsorbed water and -OH groups (Table S3). The bands at 3602.5 and 3555.2

cm^{-1} correspond to weakly hydrogen bonded water and weakly adsorbed water, respectively[9]. Other -OH related bands are 3496.0 cm^{-1} (valence vibration of hydrogen bonded -OH groups or moderately hydrogen bonded water), 3372.8 cm^{-1} (intramolecular hydrogen bonded -OH stretching), 3280.2 cm^{-1} (-OH intramolecular and intermolecular stretching modes), and 3149.5 cm^{-1} (strongly hydrogen bonded water). Beside the bands in 3700-3000 cm^{-1}, the band at 1652.3 cm^{-1} is also related to -OH vibration (i.e., -OH bending in adsorbed water and -OH bending affected by water absorption)[10]. To compare the changes of -OH related bands under different treatment conditions, the band at 1511.5 cm^{-1} (aromatic skeleton stretching vibrations) is selected as a reference since it is the strongest and most stable functional group in the lignin structure[11, 12].

We first studied the effects of moisture content on the structural changes of lignin samples during foaming. The FTIR spectra of kraft lignin samples with different moisture contents are shown in Figure 1a. The intensity ratios of adsorbed water and -OH group bands to the band of aromatic skeleton (1511.5 cm^{-1}) are calculated, normalized, and plotted in Figure 1b. It shows that the samples with decreasing moisture contents from 7.4% to 0.5% resulted in decreasing band intensities of adsorbed water and -OH groups in kraft lignin. The intensities of the bands related to the adsorbed water (3602.5, 3555.2, and 1652.3 cm^{-1}) attenuated faster than those of bands assigned to hydroxyl groups (3496.0, 3372.8, 3280.2, and 3149.5 cm^{-1}). With the decrease in moisture contents (from 7.4% to 0.5%), the band intensities are reduced in the order of $I_{3602.5}>I_{3555.2}>I_{1652.3}>I_{3149.5}>I_{3280.2}>I_{3372.8}>I_{3496.0}$, indicating that chemically bonded hydroxyl groups are relatively stable compared to adsorbed water.

TG, DTG, and DSC curves for the kraft lignin powder dried under different temperatures are shown in Figure 2. The TG/DTG curves obtained for kraft lignin show two-stage weight loss in the study temperature range (30-240 °C). The first stage (30-130 °C) is characterized by a mass

loss due to evaporation of adsorbed moisture; the peak temperatures of this stage were between 70-82 °C for lignin samples with different moisture contents. The second weight loss stage (130-240 °C) is mainly attributed to dehydration of chemically bonded water and hydroxyl groups in lignin. According to the FTIR results, the band associated with hydroxyl groups was attenuated significantly due to dehydration reactions when lignin was heated to 200 °C and higher [13], while other functional groups remained unchanged. It is noticed in Figures 2a-b that the TGA/DTG curves of four lignin samples with moisture of 2.2% or above (KL25-KL100) show very similar thermal behaviors, while KL125, and KL150 samples demonstrate different TG/DTG plots between 130-240 °C. Due to low or no moisture contents, the KL125 and KL150 samples may have undergone partial dehydration reactions under the drying condition. Furthermore, KL150 (0% moisture content) was dried above the glass transition temperature of kraft lignin (T_g = ~145) [14] which led to changes in both the thermal properties and structure of kraft lignin.

The DSC curves for kraft lignin samples also show two-stage heat flow in the temperature range of 30-240 °C. The first stage (30-130 °C) is characterized by an endothermic heat flow due to evaporation of adsorbed moisture. The second heat absorbing stage (130-240 °C) is mainly attributed to dehydration of chemically bonded water and hydroxyl groups in lignin.

The effects of cold-press pressure (0-500 psi) on the structural changes of lignin were studied using KL25. Cold pressing pressure did not significantly change lignin chemistry since the intensity ratios of the selected band to that of the aromatic skeleton band (1511.5 cm^{-1}) remained constant across different pressing pressures (Figure 3b)[11]. The TG/DTG curves show three stages of weight loss (Figures 4a-b). The first stage of weight loss from 30-130 °C was due to evaporation of adsorbed moisture. Water vapor was transported through dense materials mainly by the differential pressure across the solid body. The water vapor pressure gradient was affected by

factors like porosity, geometry, size, complexity of pores, pore shape, and pore size distribution [15]. It was observed that the peak temperature of this stage increased with increasing cold press pressure, starting at 76.2 °C for 0 psi (no pressing), 80.0 °C for 75 psi, 85.8 °C for 150 psi, 86.9 °C for 300 psi, and 91.1 °C for 500 psi. This shift in the peak is due to higher press pressures leading to more compact lignin solids with fewer and smaller pores or tunnels for transport of moisture in the densified lignin. The adsorbed water remained in the compact lignin block even when heating the sample over the boiling point of water. For the sample pressed at 500 psi, the evaporation of the adsorbed water continued above 150 °C. Weight loss during heating also decreased with increasing pressing pressure, further proving the densified sample helped to trap the moisture during the baking process. The second weight loss stage (130-195 °C) was mainly attributed to dehydration of chemically bonded water and hydroxyl groups in lignin. DTG curves (Figure 4b) show that the weight loss peaks become narrower and shift to lower temperatures with increasing cold press pressure. As the dominant functional group, hydroxyl groups can be categorized into phenolic and aliphatic hydroxyl groups. Dehydration reactions between these hydroxyl groups in lignin can occur intra- and inter- molecularly. The dehydration of hydroxyl groups is affected by several factors like the types, the density, the location of hydroxyl groups in the molecule, and the distance between the adjacent hydroxyl groups. Figure 4b shows no obvious weight loss peaks between 130-195 °C for the loose lignin powder samples, indicating the dehydration reaction is promoted in the pressed samples since the density of hydroxyl groups is increased. The increased density decreases the distance between the hydroxyl groups and lowers the activation energy, allowing –OH groups to dehydrate more easily and shifts the dehydration to lower temperature. The dehydration reaction may mainly occur intramolecularly, with minor intermolecular reactions in loose or less densified samples, while the reaction in the adequately pressed lignin samples may

have a comparatively higher intermolecular reaction component. Due to the prevalent dehydration of the pressed lignin at 130-195 °C, a considerable amount of water can be formed as steam. This high steam level helps decrease the softening temperature of lignin [16]. Decreasing the softening temperature allowed more steam to be trapped, resulting in less water loss from the lignin matrix. The third weight loss stage (195-240 °C) is mainly attributed to the dehydration of hydroxyl groups in lignin and the release of trapped steam bubbles in the softened lignin matrix. With increasing the baking temperature from 195 to 240 °C, more hydroxyl groups are dehydrated to form steam, causing the steam bubbles in the softened lignin to continue expanding. When the steam pressure in the bubbles is high enough, it will break through the softened lignin body and generate a foam structure with interconnected gas channels.

The sample loading also affects structural change. The higher a sample loading was, the smaller heat and mass transfer areas resulted [1]. Moisture transfer distance also increased with increase in sample loading. Therefore, it is obvious that increasing the sample loading decreased the moisture transport and evaporation rate as reflected by the shift of weight loss peaks associated with moisture evaporation to higher temperature in DTG curves (Figure S2). However, sample loading did not affect the –OH group dehydration temperature in lignin.

3.2. Characteristics of lignin foams

Table 1 lists the density and compressive strength of the lignin foams prepared from kraft lignin cold-pressed at 150 psi. The bulk densities of the foams (LF25, LF50, LF75, LF100, LF125, and LF150) are 0.21, 0.25, 0.27, 0.30, 0.37 and 0.83 g/cm^3, respectively. It should be noted that decreasing lignin moisture content led to an increase in the foam density. Similarly, increased amounts of lignin also correspond to increased foam density. A lower moisture content results in less steam trapped in the softened lignin. Less blowing agent (steam) obstructs the expansion of

lignin to create a less porous structure, therefore, the bulk density of lignin foam increases with decreased moisture contents. For the sample dried at 150 °C (KL150), all adsorbed moisture evaporated, and the hydroxyl groups partially dehydrated, leading to a non-foamed product with a bulk density of 0.83 g/cm^3, similar to that of the pressed lignin block (0.85-0.88 g/cm^3).

SEM images of lignin foams are shown in Figure 5&S3. The foams exhibited open cell structure. The pores were interconnected because the expanding steam bubbles in the softened lignin ruptured the thin walls between the bubbles. LF125 had the most uniform porous structure with the smallest average pore size (152.2 μm) among all the five samples (Figure 5e). In contrast, LF50, LF75 and LF100 showed less uniform pore distributions with smaller sizes (Figures 5b-d). Their respective average pore sizes were 345.6, 342.1, 237.4 μm (Figure6). When the foam was made of lignin with further increased (LF25) or reduced (LF150) moisture (7.4% and 0%, respectively), the porous structures were not desirable. LF25 showed a nonuniform porous structure with a wide range of pore sizes from 100 to over 1000 μm (Figure 5a), whereas LF150 was still solid, with no pore structures formed (Figure 5f). The porosity and pore size distribution might be predominantly controlled by the adsorbed water in lignin, which acts as the major source of the steam blowing agent during foaming, for making the LF25, LF50, and LF75 foams. Both adsorbed and dehydrated water acted as the blowing agent for LF100. Dehydrated water served as the majority of blowing agent for LF125. The porosity of lignin foam decreased with decreasing moisture contents in the feedstock. Low moisture content yields fewer and smaller steam bubbles in the softened lignin, which results in lower porosity of the foam products. This agrees with the trend of foam densities (Table 1).

The mechanical properties of LF materials depend on the initial precursor compositions, densities of the foams, and microstructural arrangement in the foams[17]. The compressive strengths

of the foams (LF25, LF50, LF75, LF100, LF125, and LF150) are measured as 1.18, 1.51, 1.62, 1.87, 2.47 and 6.36 MPa, respectively (Table 1). The compressive strengths of the lignin foams increase with decreasing lignin moisture contents because this strength is proportional to the density. Young's modulus showed a similar trend to compressive strength and increased from 25.2 to 54.8 MPa when the moisture content of lignin for foaming decreased from 7.4% to 0.5%. Foams with lower densities exhibit higher porosity but lower compressive strength and Young's modulus [18]. Compared to commercial foam products, the density and compressive strength of the lignin foams are also higher than those of commercial polystyrene (PS) foams[19] and are comparable to the phenolic-based polyurethane (PU) foams [20] (Table S4). Moreover, the foams showed good thermal insulation property (Table 1&S4). Thermal conductivities as low as 0.035 W/mK were obtained from LF25. With relatively uniform pore structure, LF125 also showed a lower thermal conductivity (0.043 W/mK).

Based on thermal insulation properties and compressive strengths that are comparable to or better than commercial petrochemical-based foams (Table S4), lignin foam shows great promise as structural insulated panel (SIP) core material, yielding a SIP that is a potentially carbon negative building material. The manufacturing process was scaled up to make large size (LF75) lignin foam (Figure 7a). These lignin foams were used as the composite core for a structural insulated panel (SIP) with a dimension of 16" wide × 64" long × 4" thick (Figure 7b). This prototyping for scaled-up production is a critical step to go beyond the proof concept and toward commercialization. In future work, the lignin-based SIP will be fully investigated for building performance and code requirements.

3.3. Possible mechanisms for lignin foaming and stabilization

To create a cellular structure, a blowing agent must be used during a foaming process[21]. Blowing agents can be categorized into physical blowing agents (PBAs) and chemical blowing agents (CBAs) based on origins of gas for foaming [22]. In the lignin foaming process of this work, water vapor is the proposed blowing agent. Prior studies also reported using water as both a blowing agent and plasticizer of starch-based foam in a baking process [23]. During the preparation of starch-based foam, when the temperature is higher than the boiling point of water, some of the water contained in the starch-based materials becomes gaseous and creates bubbles. The remaining water acts as a plasticizer to gelatinize the starch and provide melting strength, enabling the expansion of the starch-based materials to form a foam structure. It was reported that water is adsorbed by Van der Waals bonds or by electrostatic forces over wood-based polymers when the moisture content is over 6%, and the adsorbed moisture forms a multi-molecular water layer which makes a non-unform distribution of water in wood, lignin, or cellulose [24]. This non-uniform distribution of water can explain the non-uniform pore size distribution observed in the LF25 foam, which had greater than 6% moisture content. When the moisture content is below 6%, water molecules are linked by H-bonds of functional groups in cellulose or lignin, forming a mono-molecular layer [24]. Therefore, water molecules in lignin containing less than 6% moisture content could be more evenly distributed among functional groups in the lignin when its moisture content is reduced. This could explain the more uniform pore size and pore size distribution of the lignin foams when water was reduced to a lower and more optimal level.

Lignin is composed of an aromatic skeleton containing numerous functional groups like hydroxyl (both phenolic and aliphatic), methoxyl, carbonyl, and carboxyl groups. These functional groups are hydrophilic and act as adsorption sites by forming hydrogen bonds with water, allowing lignin to adsorb water molecules [25]. The physiochemical properties of lignin are significantly

affected by its moisture content [26]. In the current work, it is proposed to foam kraft lignin using the adsorbed water as the blowing agent through a thermal process. Softening temperatures of lignin range from 127-193 °C [27], however, kraft lignin will not soften and melt until over 150 °C and higher [28]. Thus, it is very important to trap water vapor in lignin until the lignin softens or melts. The factors influencing gas diffusion includes the matrix's porosity, bulk density, diffusing gas species, and aggregate size [29]. To trap moisture while elevating temperature, we thus compressed lignin into a compact lignin block at room temperature. This compact lignin block had high bulk density and low porosity, which restricted the movement of gas and water in the confined dense lignin block. When heating the compact lignin under an elevating temperature, significant water vapor should be trapped until the lignin reaches softening or melting temperature. The trapped water vapor served as the blowing agent to bubble and foam the softened/melting lignin.

Besides the adsorbed water which can serve as a physical blowing agent for lignin feedstock, another water resource may be generated by dehydration reactions between two adjacent –OH groups in lignin. Dehydration reactions of lignin usually occur in the temperature range of 100 –200°C, while crosslinking/condensation reactions simultaneously occur to form large molecules. Water from the dehydration reaction of –OH groups is a type of chemical blowing agent in the lignin foaming process. Dehydration can occur during the cross-linking/polymerization of lignin molecules, first by the heat-generating auto-polymerization between lignin molecules and later by reaction of free –OH groups of lignin molecules under thermal conditions [30]. The foaming or bubble formation inside the lignin foam is created by vaporizing either the moisture adsorbed in lignin, or the water generated through dehydration/cross linking reactions.

Based on the role of water in lignin foaming discussed above, we propose the possible foaming mechanism illustrated in Scheme 2. There are three major stages involved in foaming. First, the compact lignin matrix swells when heated from room temperature to 130 °C [31] and the physically adsorbed moisture diffuses inside the lignin matrix as shown in TGA and DSC results (Figures 2&4). Then, when further increasing the baking temperature from 130 to 200 °C, the lignin block undergoes the softening/melting process, and the adsorbed moisture vaporizes and creates steam vesicles inside the softened lignin matrix [24]. Some adjacent hydroxyl groups in the lignin are dehydrated, releasing water which joins the adsorbed water in the steam vesicles in the softened lignin matrix (supported by TGA and FTIR results). Intra- and inter-molecular cross-linking/condensation reactions simultaneously occur between lignin molecules, furthering the polymerization process of kraft lignin. At the final stage, further increasing the heating temperature from 200 to 240 °C, more hydroxyl groups are dehydrated to form steam. This causes the steam bubbles in the softened lignin to continue expanding while the viscosity of the melted/softened lignin decreases. The bubbles break through the lignin matrix when the steam pressure in the bubbles is high enough (DSC data, Figure 2), resulting in a softened lignin foam with interconnected gas channels. With continuing polymerization caused by dehydration/cross-linking reactions, more high molecular weight fractions are formed during the foaming process, causing an increase in viscosity of the lignin block and initializing solidification of the lignin foam. A rigid lignin foam with open cell structure is achieved when the foamed lignin matrix is cooled to room temperature.

4. Conclusions

Rigid foams were prepared from Kraft lignin as the sole source through baking-based eco-foaming. The lignin foam precursors are first compressed into a lignin block in a mold, then the

lignin block is heated to generate a lignin foam at a temperature range of 200-240 °C. The foams showed a density of 0.21- 0.37 g/cm^3, porosity of 81- 94%, average pore size ranges from 152.2 to 347.2 μm, compressive strength of 1.18 MPa – 6.36 MPa, and thermal conductivity of 0.035-0.048 W/mK. Moisture content in the feedstock can be used to control the pore structure of the lignin foam. LF25 shows a wide range of pore sizes, and the nonuniform distribution may be due to the high moisture content (7.4%) and inhomogeneous distribution of water in KL25. With decreasing moisture contents, the pore structure becomes more uniform. The average pore sizes might be predominantly controlled by the origin of the steam blowing agent. For LF25, LF50, and LF75, adsorbed moisture (7.4-1.4%) may be the major source of the steam blowing agent during the foaming process. Both the adsorbed moisture and the dehydrated water contribute as the blowing agent for LF100, while the dehydrated water serves as the majority blowing agent for LF125. The lignin foam materials have many potential applications associated with their unique properties such as core insulation materials of structural insulated panels (SIPs).

Acknowledgements

This work was supported by the USDA Forest Service through Grant Nos. 19-JV-11111124-053, 19-JV-11111124-063, 20-JV-11111124-035, and Wood Innovations (Grant No. 20-DG-11094200-234). The authors would like to thank Domtar Corp for providing kraft lignin. Special thanks to Joseph Destree, Joshua Limbaugh, Kimberly Hoxie, CR Boardman, Sara J. Fishwild, Marshall M. Begel, and Will Kinney at USDA Forest Products Laboratory, for their help in making this project run successfully.

References

1. F. Asdrubali, F. D'Alessandro and S. Schiavoni, *Sustainable Mater. Technol.*, 2015, **4**, 1-17.
2. *US Patent,* 6125608A, 2000.
3. D. Bajwa, G. Pourhashem, A. H. Ullah and S. Bajwa, *Ind. Crops Prod.*, 2019, **139**, 111526.
4. V. Mimini, V. Kabrelian, K. Fackler, H. Hettegger, A. Potthast and T. Rosenau, *Holzforschung*, 2018, **73**, 117-130.
5. Q. Yan, R. Arango, J. Li and Z. Cai, *Mater. Des.*, 2021, **201**, 109460.
6. *US Patent,* 20190248656A1, 2021.
7. ASTM-C578-23, *Standard Specification for Rigid, Cellular Polystyrene Thermal Insulation*, 2023.
8. ISO22007-2, *Determination of thermal conductivity and thermal diffusivity*, 2022.
9. M. Báder, R. Németh, J. Sandak and A. Sandak, *Cellulose*, 2020, **27**, 6811-6829.
10. M. Kačuráková, P. S. Belton, R. H. Wilson, J. Hirsch and A. Ebringerová, *J. Sci. Food Agric.*, 1998, **77**, 38-44.
11. O. Faix, *Holzforschung*, 1991, **45**, 21-28.
12. X. Guo, Y. Wu and N. Yan, *Wood Sci. Technol.*, 2018, **52**, 971-985.
13. N. Mahmood, Z. Yuan, J. Schmidt and C. C. Xu, *Bioresour. Technol.*, 2013, **139**, 13-20.
14. H. Jeong, J. Park, S. Kim, J. Lee, N. Ahn and H. Roh, *Fibers Polym.*, 2013, **14**, 1082-1093.
15. M. Lawrence and Y. Jiang, *Bio-aggregates based building materials: state-of-the-art report of the RILEM technical committee 236-BBM*, 2017.
16. W. Cousins, *Wood Sci. Technol.*, 1976, **10**, 9-17.
17. S. Li, Y. Song, Y. Song, J. Shi, L. Liu, X. Wei and Q. Guo, *Carbon*, 2007, **45**, 2092-2097.
18. X. Meng, J. Xu, J. Zhu, Z. Li, J. Zhao, M. J. Reece and F. Gao, *Journal of the American Ceramic Society*, 2020, **103**, 6088-6095.
19. L. Ravindran, M. Sreekala, S. Anilkumar and S. Thomas, *Thermal Stability of Phenolic Foams*, 2022.
20. Q. Xu, R. Gong, M. Cui, C. Liu and R. Li, *High Perform. Polym.*, 2015, **27**, 852-867.
21. W. Yamsaengsung and N. Sombatsompop, *Composites, Part B*, 2009, **40**, 594-600.
22. G. Coste, C. Negrell and S. Caillol, *Eur. Polym. J.*, 2020, **140**, 110029.
23. L. Meng, H. Liu, L. Yu, Q. Duan, L. Chen, F. Liu, Z. Shao, K. Shi and X. Lin, *Ind. Crops Prod.*, 2019, **134**, 43-49.
24. I. Hartley, F. Kamke and H. Peemoeller, *Wood Sci. Technol.*, 1992, **26**, 83-99.
25. Z. Gao, Y. Ding, W. Yang and W. Han, *J. Mol. Model.*, 2017, **23**, 1-19.
26. N. Volkova, V. Ibrahim, R. Hatti-Kaul and L. Wadsö, *Carbohydr. Polym.*, 2012, **87**, 1817-1821.
27. D. Goring, in *Consolidation of the Paper Web*, 1965, vol. 1, pp. 555-575.
28. H. Jeong, J. Park, S. Kim, J. Lee and J. W. Cho, *Fibers Polym.*, 2012, **13**, 1310-1318.
29. A. R. Grable and E. Siemer, *Soil Sci. Soc. Am. J.*, 1968, **32**, 180-186.
30. T. Varila, H. Romar, T. Luukkonen, T. Hilli and U. Lassi, *Heliyon*, 2020, **6**.
31. B. Jiang, C. Chen, Z. Liang, S. He, Y. Kuang, J. Song, R. Mi, G. Chen, M. Jiao and L. Hu, *Adv. Funct. Mater.*, 2020, **30**, 1906307.

Figure captions

Scheme 1. Fabrication process of foams from kraft lignin.

Scheme 2. Possible foaming mechanism of kraft lignin by a baking process.

Figure 1. FTIR spectra (a) and the water and hydroxyl group-related band intensity ratio (b) of kraft lignin samples dried at different temperatures.

Figure 2. Thermal properties of kraft lignin dried at different temperatures: (a) TG, (b) DTG, and (c) DSC.

Figure 3. FTIR spectra (a) and the water and hydroxyl group-related band intensity ratio (b) of kraft lignin samples cold pressed at different pressures.

Figure 4. Thermal properties of kraft lignin powder cold pressed at different pressures: (a) TG, (b) DTG, and (c) DSC.

Figure 5. SEM images of lignin foam specimens under 50× magnification; (a) LF25, (b) LF50, (c) LF75, (d) LF100, (e) LF125, and (f) LF150.

Figure 6. Pore size distribution in lignin foams prepared from kraft lignin dried at different temperatures.

Figure 7. (a) A lignin foam sample with dimensions of 16" wide × 36" long ×5" thick. (b) A finished SIP sample with lignin foam core (16" wide × 64" long × 4" thick).

Table 1. Characteristics of lignin foams

Lignin foam	**Porosity (%)**	**Average pore size (μm)**	**Density (g/cm^3)**	**Compressive strength (MPa)**	**Young's modulus (MPa)**	**Thermal conductivity (W/m·K)**
LF25	94.0	347.2	0.21±0.03	1.18±0.16	25.2 ± 1.7	0.03±0.003
LF50	90.9	345.6	0.25±0.02	1.51±0.13	35.6 ± 2.5	0.035±0.002

LF75	87.8	342.1	0.27±0.02	1.62±0.15	36.2 ± 2.3	0.038±0.003
LF100	83.4	237.4	0.30±0.02	1.87±0.18	40.3 ± 3.6	0.043±0.003
LF125	81.2	152.2	0.37±0.03	2.47±0.21	54.8 ± 4.9	0.052±0.004
LF150	N/A	N/A	0.83±0.03	6.36±0.19	120.5 ± 8.2	0.081±0.002

N/A: no pores.

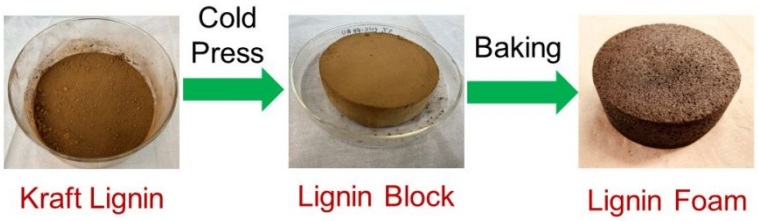

Scheme 1. Fabrication process of foams from kraft lignin.

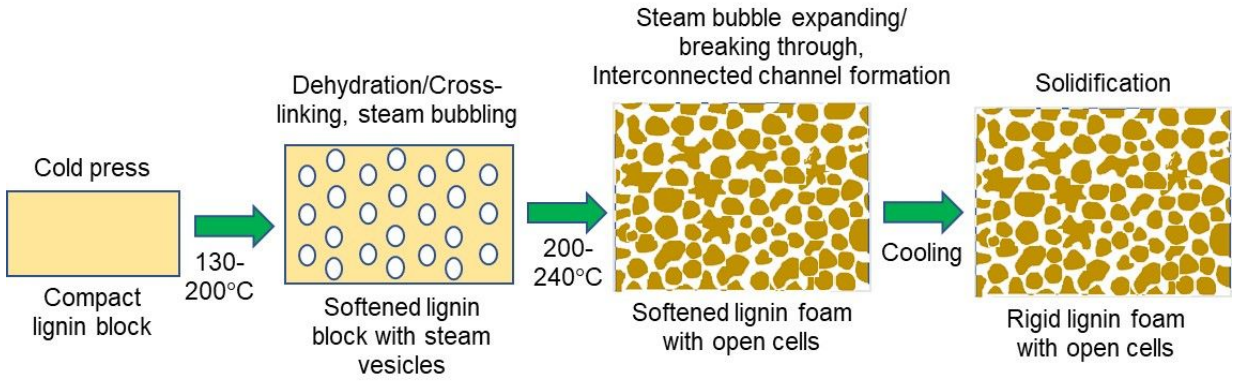

Scheme 2. Possible foaming mechanism of kraft lignin by a baking process.

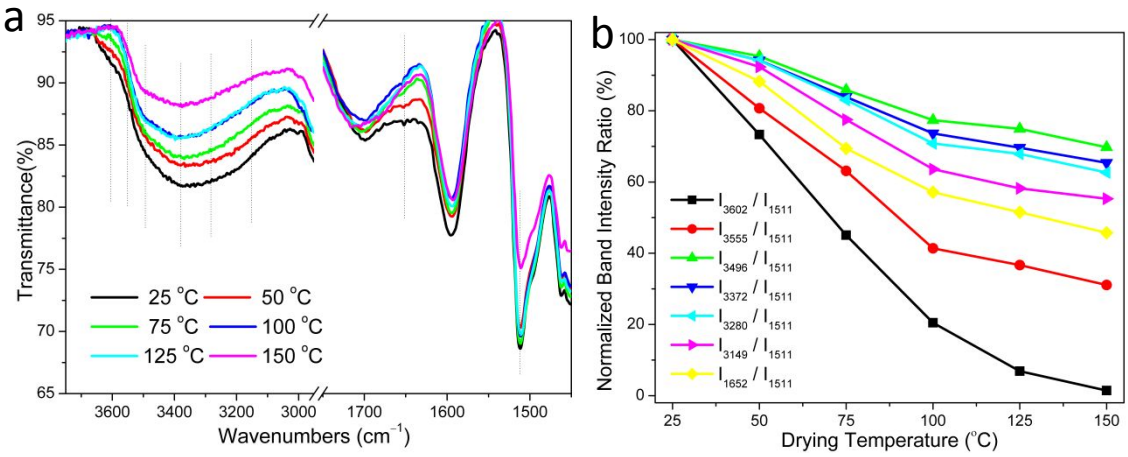

Figure 1. FTIR spectra (a) and the water and hydroxyl group-related band intensity ratio (b) of kraft lignin samples dried at different temperatures.

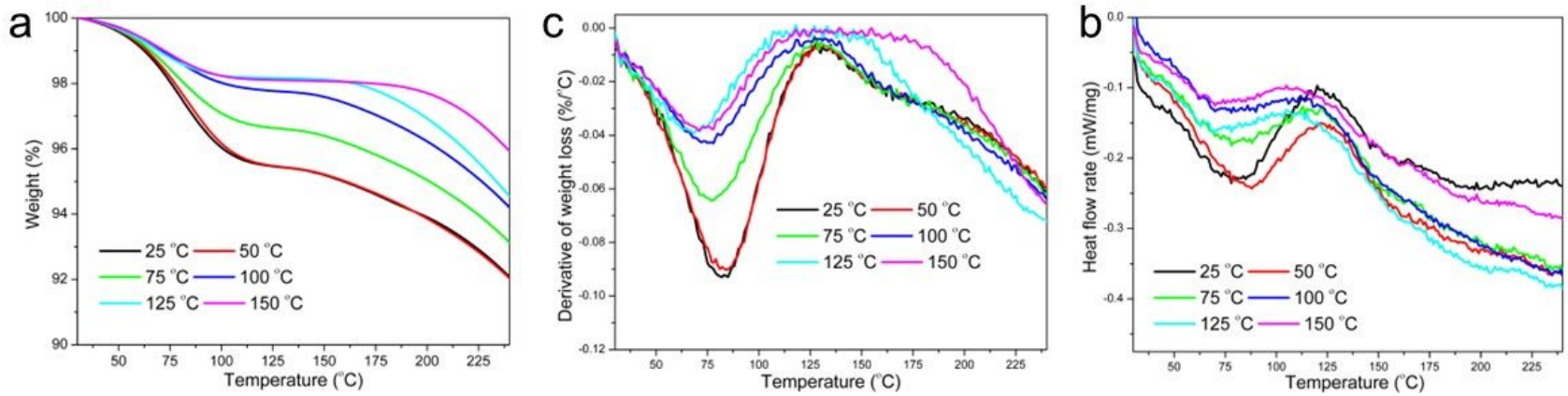

Figure 2. Thermal properties of kraft lignin dried at different temperatures: (a) TG, (b) DTG, and (c) DSC.

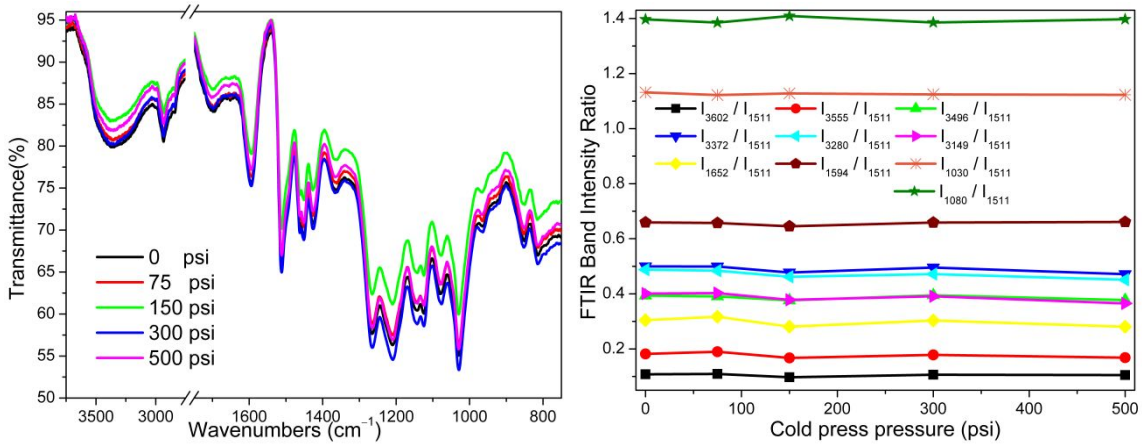

Figure 3. FTIR spectra (a) and the water and hydroxyl group-related band intensity ratio (b) of kraft lignin samples cold pressed at different pressures.

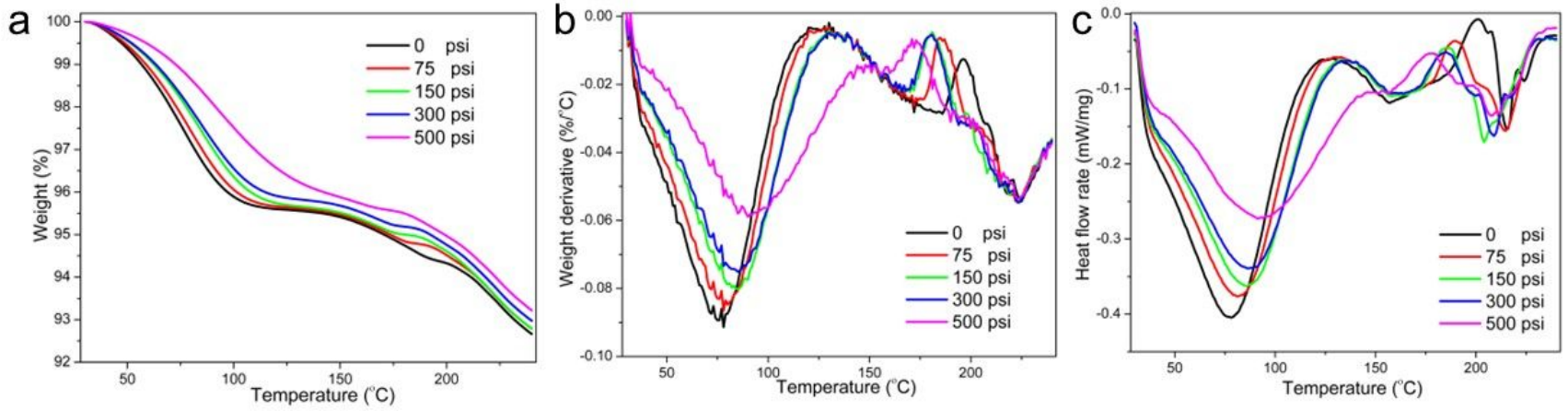

Figure 4. Thermal properties of kraft lignin powder cold pressed at different pressures: (a) TG, (b) DTG, and (c) DSC.

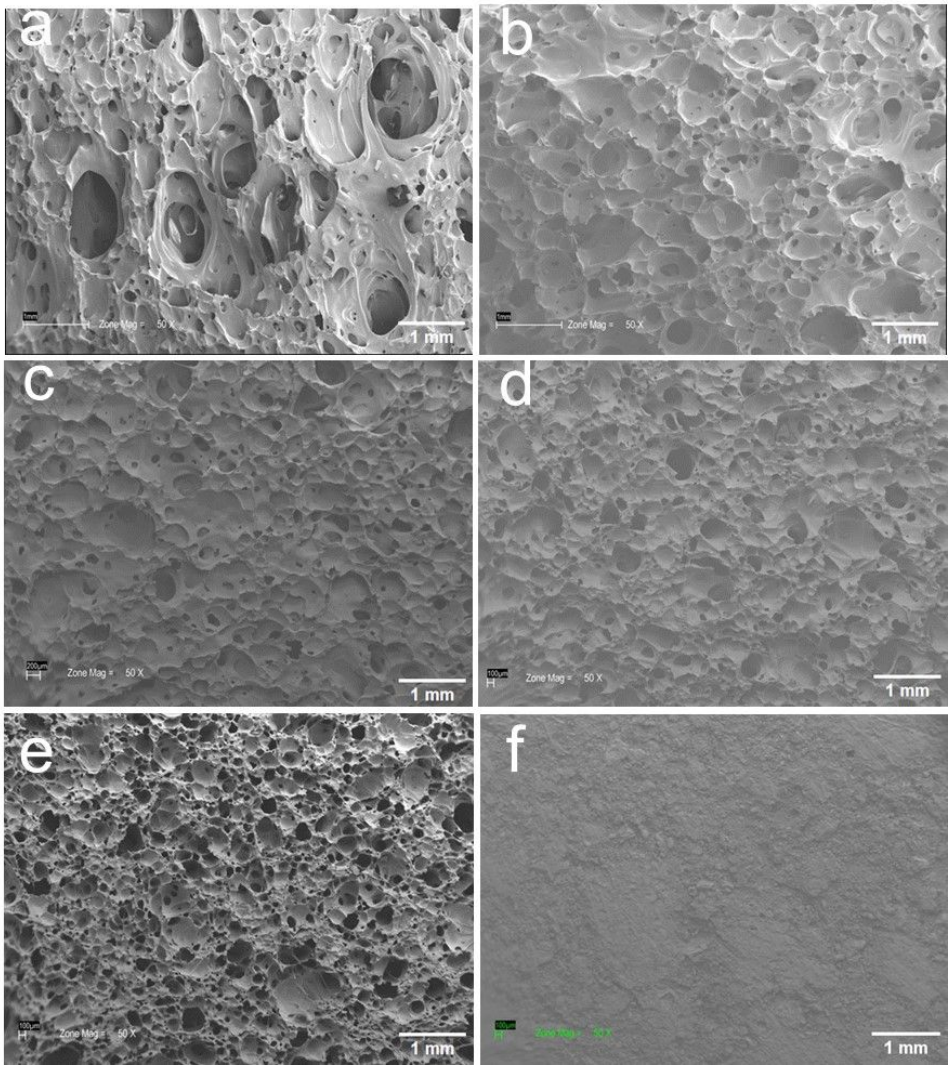

Figure 5. SEM images of lignin foam specimens under 50× magnification; (a) LF25, (b) LF50, (c) LF75, (d) LF100, (e) LF125, and (f) LF150.

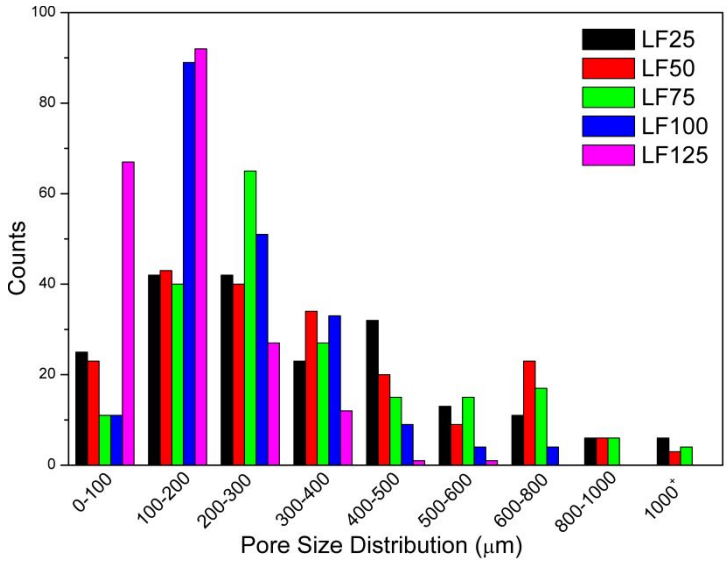

Figure 6. Pore size distribution in lignin foams prepared from kraft lignin dried at different temperatures.

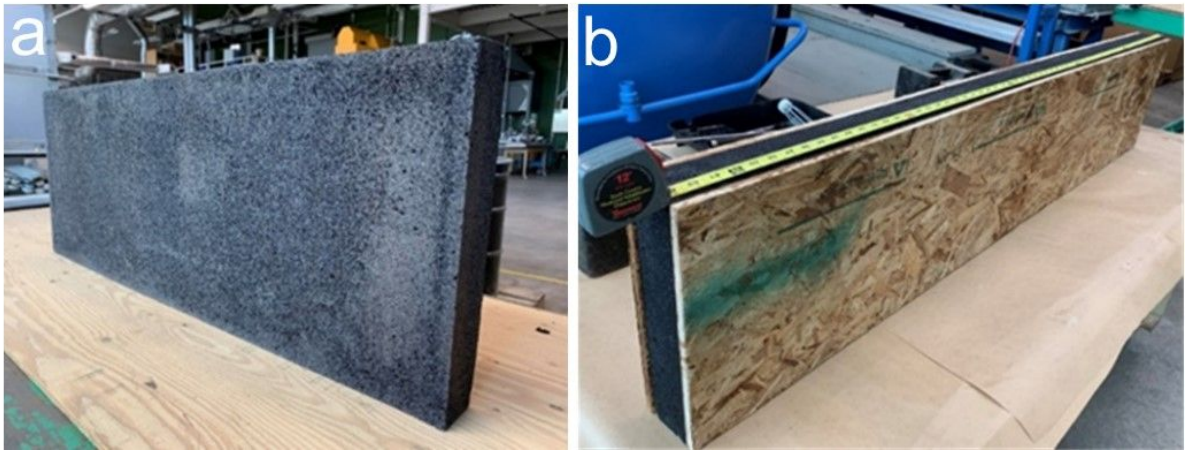

Figure 7. (a) A lignin foam sample with dimensions of 16" wide × 36" long ×5" thick. (b) A finished SIP sample with lignin foam core (16" wide × 64" long × 4" thick).